3-1-2022

Large-field magnetoresistance of nanometer scale nickel films grown on molybdenum disulfide

Timothy E. Kidd
University of Northern Iowa

Paul M. Shand
University of Northern Iowa

See next page for additional authors

Large-field magnetoresistance of nanometer scale nickel films grown on molybdenum disulfide

Cite as: AIP Advances **12**, 035233 (2022); https://doi.org/10.1063/9.0000291
Submitted: 31 October 2021 • Accepted: 09 December 2021 • Published Online: 15 March 2022

Timothy E. Kidd, Paul M. Shand, Andrew Stollenwerk, et al.

Large-field magnetoresistance of nanometer scale nickel films grown on molybdenum disulfide

Cite as: AIP Advances 12, 035233 (2022); doi: 10.1063/9.0000291
Presented: 27 December 2021 • Submitted: 31 October 2021 •
Accepted: 9 December 2021 • Published Online: 15 March 2022

Timothy E. Kidd,[a] Paul M. Shand, Andrew Stollenwerk, Colin Gorgen, Young Moua, Lukas Stuelke, and Pavel V. Lukashev

AFFILIATIONS

Department of Physics, University of Northern Iowa, Cedar Falls, Iowa 50614-0150, USA

Note: This paper was presented at the 15th Joint MMM-Intermag Conference.
[a]**Author to whom correspondence should be addressed:** tim.kidd@uni.edu.
URL: https://chas.uni.edu/physics/directory/tim-kidd

ABSTRACT

The magnetoresistance of thin nickel films grown on molybdenum disulfide was measured in perpendicular magnetic fields as high as 90 kOe. Films with thicknesses of 20 nm provided continuous surfaces for measurement. The magnetoresistance was found to be linear with respect to the applied magnetic field with no sign of saturation. There was also no evidence of hysteresis or temperature dependence between 100 to 300 K. STM measurement showed the deposited Ni forms a continuous film of extremely small nanoclusters. However, the field dependence of magnetoresistance was found to be significantly larger than bulk Ni, which is in turn larger than Ni with nanoscale grains. We expect the unusual magnetoresistance behavior to arise from some property of the Ni-MoS_2 interface.

I. INTRODUCTION

Understanding the fundamental properties of thin ferromagnetic films is important for developing new technologies in spintronics and related areas.[1,2] Being able to manipulate the properties of materials using the emergent physics of nanoscale materials, or by determining the threshold for bulk-like behavior are both important aspects of such research. The properties of ultrathin ferromagnetic films can deviate significantly from their bulk counterparts.[3,4]

Molybdenum disulfide is a layered semiconducting material with high interest for its electro-optical properties,[5] especially in single or finite layer form as a semiconducting analog to graphene.[6,7] MoS_2 also presents an interesting substrate for the growth of metal films. Its relatively inert van der Waals terminated surface bonds weakly to deposited metals and allows for significant adatom diffusion. The weak interfacial bonding also reduces the importance of strain induced by lattice mismatch, which is considerable for most metals and is about 20% for Ni/MoS_2. Transmission electron microscopy studies have shown that a variety of FCC metals can grow epitaxially on MoS_2, despite the large lattice mismatch, although Ni is not among them.[8]

Our own studies have shown that several noble metals display electronic growth to create novel quantized nanometer scale films on MoS_2.[9–11] However, our recent density functional theory (DFT) calculations show no evidence for quantization in the density of states for Ni/MoS_2.[12] Instead, the calculations show the Ni electronic structure is very bulk-like even for a 6 atomic layer film. Interestingly, the metallic character and spin polarization of the Ni film extends into the uppermost MoS_2 layer, with underlying MoS_2 layers maintaining bulk semiconducting properties. In this work, we explore the structural and magneto-transport properties of Ni films grown on MoS_2 to determine potential for device applications.

II. METHODS

A. Film growth and microscopy

Samples were prepared by depositing Ni onto the cleaved surface of commercially available MoS_2 (SPI supplies) in a vacuum chamber with a base pressure of 5×10^{-10} mbar. Deposition occurred at room temperature using a 2 mm Ni wire (99.995% pure) in a mini electron-beam evaporator (MANTIS QUAD-EV). A flux monitor was used to maintain a consistent deposition rate. The deposition rate was calibrated from resulting scanning tunneling

microscopy images (STM). The error in determining film thickness from the STM images is estimated to be ±20%. Thinner nickel films, on the order of 2 nm, were deposited onto MoS_2 crystals fixed to sample holders appropriate for STM measurements. Prepared samples were transferred *in situ* to the adjacent variable temperature STM head (Omicron). STM tips were mechanically cut from a 0.25 mm $Pt_{90}Ir_{10}$ wire. Scanning parameters used in this study were relatively consistent. The tunneling bias typically ranged from 0.75 to 1.5 V and the current set point varied from 0.5 to 5 nA. No significant differences were observed between extremal scanning parameters. Thicker Ni films, on the order of 20 nm, were deposited onto MoS_2 affixed to glass slides for magnetoresistance measurements. Between growth and transport measurements, the samples were exposed to ambient conditions for several hours. This exposure is known to induce the formation of a surface oxide layer, but one which is less than 3 nm thick.[13]

B. Magnetoresistance measurements

Resistance measurements were performed with a Quantum Design DynaCool PPMS system using the Electrical Transport Option (ETO). The standard in-line four-point probe method was used for the measurements, with a drive current of 0.01 mA. Magnetic field strengths up to 90 kOe were applied perpendicular to the plane of the Ni film.

C. Density functional calculations

Density functional calculations were performed using the projector augmented-wave method (PAW),[14] implemented in the Vienna *ab initio* simulation package (VASP)[15] within the generalized-gradient approximation (GGA).[16] The integration method[17] with a 0.05 eV width of smearing is used, along with the cut-off energy of the plane-waves of 500 eV. Structural optimization is performed with the energy convergence criteria of 10^{-2} meV, while the total energy and electronic structure calculations are performed with a convergence criteria of 10^{-3} meV. The Brillouin zone integration of thin-film cells is performed with a k-point mesh of 6 × 6 × 1. The van der Waals interaction is included in the calculations, using the zero damping DFT-D3 method of Grimme.[18] Periodic boundary condition is imposed for all calculations. Some of the results and figures are obtained using the MedeA® software environment.[19] Most of the calculations are performed using Extreme Science and Engineering Discovery Environment (XSEDE) resources located at the Pittsburgh Supercomputing Center (PSC),[20] and the resources of the Center for Functional Nanomaterials (CFN) at Brookhaven National Laboratory (BNL).

III. RESULTS AND DISCUSSION

The initial stages of growth for Ni/MoS_2 are not highly uniform. The initial growth mode for Ni on MoS_2 is shown in Fig. 1. Nanometer scale Ni films are highly granular, with typical cluster sizes ranging from one to three nanometers. This creates a continuous, yet inhomogeneous, film.

In comparison to the growth of Au or other noble metals on MoS_2, Ni behaves far differently. Noble metals exhibited electronic growth modes resulting in quantized length scales and atomically flat nanostructures.[9–11] The Ni clusters are instead highly rounded, displaying a Volmer-Weber growth mode.

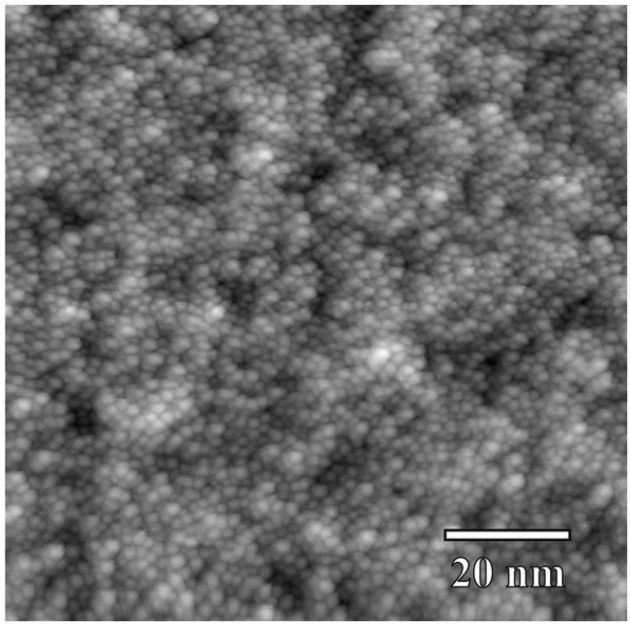

FIG. 1. STM topography of 2nm thick Ni film deposited at room temperature on MoS_2. System forms interconnected clusters with typical sizes ranging from 1-3 nm.

The differences in growth modes between Ni and the noble metals Pd, Ag, and Au can be related to differences in binding energies and lattice mismatch. Figure 2 compares these quantities as calculated by DFT. Here, the binding energies, $E_{binding}$ are calculated as follows:

$$E_{binding} = E_{metal/MoS_2} - E_{metal} - E_{MoS_2}.$$

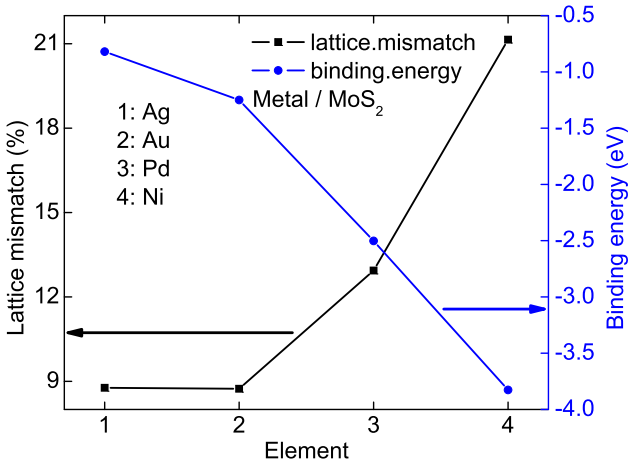

FIG. 2. Calculated lattice mismatch (black line and squares), and binding energies (blue line and circles) of Ag, Au, Pd, and Ni. Atoms are numbered as indicated in the figure.

Here, E_{metal/MoS_2} is the energy of two monolayers of MoS_2 with a single metal atom placed at its surface (in the optimized geometry), E_{metal} is the energy of a single metal atom, placed in a "box," and E_{MoS_2} is the energy of two monolayers of MoS_2 in a thin film geometry.

Ni binds most strongly to the MoS_2 surface and has the largest lattice mismatch. In particular, the Ni-MoS_2 binding energy is around three times stronger than for Au or Ag. Thus, the relative mobility of Ni adatoms would be far less than that of the noble metals. These qualities would predict lesser film quality for the Ni/MoS_2 system and explain the formation of Ni nanoclusters.

Our large field transverse magnetoresistance measurements are shown in Fig. 3. We can see the surface oxide layer has very little impact. The zero-field resistance is about 100 Ω at room temperature, indicating metallic conduction.

Measurements were taken with the magnetic field perpendicular to the film plane (and hence the transport current). No significant hysteretic effects were seen as the field was cycled from zero to 90 kOe and back. The linear fit to data collected while ramping up and down the magnetic field is shown in Fig. 3. The fit is quite good, with an uncertainty in the slope of 2%. These results were consistent for data taken on samples anywhere from 200K to 340K. The curves were always quite linear, with no signs of saturation.

The data indicate a field dependence for the magneto-resistance of $m = -0.064\%$/kOe. This negative slope is consistent with measurements performed near room temperature in both single crystal and polycrystalline Ni films.[21] Based on the film topography seen in Fig. 1, we expect the magneto-resistance to behave similarly to Ni with nanoscale grains. Interestingly, measurements performed by Isnaini *et al.* indicate the field dependence weakens with smaller grain sizes.[22] Ni foils with tens of nanometer grain sizes had $m \approx -0.01\%$/kOe, micrometer grain size had $m \approx -0.02\%$/kOe, and bulk Ni results with $m < -0.03\%$/kOe. Given magnetoresistance tends to decrease with decreasing grain size, there appears to be a different origin for the relatively high field dependence seen in our magnetoresistance measurements.

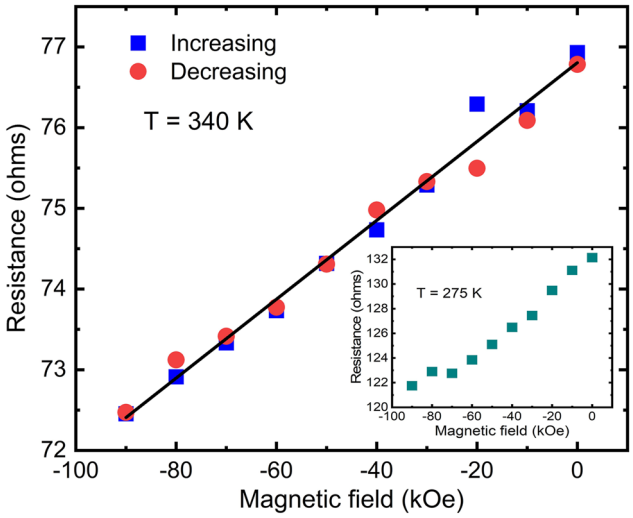

FIG. 3. Transverse magnetoresistance measurements on a 20 nm thick Ni film grown on an MoS_2 substrate.

As seen in the inset of Fig. 3, the resistance tends to increase at lower temperatures. This is consistent with semiconducting behavior and indicates the MoS_2 substrate has a significant contribution to the transport properties of the system. However, pure MoS_2 does not show significant magnetoresistance effects for fields up to 8 T.[23] However, this same study showed the inclusion of a graphene layer at the MoS_2 surface induced significant, and non-saturating, magnetoresistance behavior below 150 K. The magnetoresistance of disordered semiconductors can behave similarly to our measurements of the Ni/MoS_2 system.[24] Given the MoS_2 substrates are single crystal, any potential disorder in the substrate would have to arise at the interface.

Non-saturating magnetoresistance behavior has been seen for finite layer MoS_2 systems coupled to ferromagnetic insulators.[23] However, in this study the magnetoresistance was only significant when the MoS_2 was less than ten layers thick. Enhanced anisotropic magnetoresistance was seen in permalloy/MoS_2 bilayers,[25] with MoS_2 layers 50 nm thick, but there was no evidence for a lack of saturation in the magnetoresistance. The behavior seen here using single crystal bulk MoS_2 substrates is similar to that found in disordered and/or finite layer systems. From DFT measurments,[12] we also expect a high degree of hybridization for the MoS_2 layer in contact with Ni. Overall, this indicates the behavior seen here is influenced by characteristics of the Ni/MoS_2 interface.

IV. CONCLUSIONS

When deposited upon MoS_2, nickel forms continuous films composed of extremely small nanoclusters. Ni has a very different growth profile as compared to noble metals, which is likely due to a much stronger bonding to the substrate. The Ni films are metallic and display significant magnetoresistive behavior. Unlike previous studies on Ni solids with nanoscale domains, the field dependence for magnetoresistance is significantly larger than the bulk value. We expect the different behavior arises from some characteristic of the Ni-MoS_2 interface, but further studies are needed to accurately determine the origin of this behavior.

ACKNOWLEDGMENTS

The work is supported by Grant No. DE-SC0020334 funded by the US Department of Energy, Office of Science. This work used the Extreme Science and Engineering Discovery Environment (XSEDE), which is supported by National Science Foundation Grant Number ACI-1548562. This work used the XSEDE Regular Memory (Bridges) and Storage (Bridges Pylon) at the Pittsburgh Supercomputing Center (PSC) through allocation TG-DMR180059, and the resources of the Center for Functional Nanomaterials, which is a US DOE Office of Science Facility, and the Scientific Data and Computing Center, a component of the Computational Science Initiative, at Brookhaven National Laboratory (BNL) under Contract No. DE-SC0012704.

AUTHOR DECLARATIONS

Conflict of Interest

The authors have no conflicts to disclose.

DATA AVAILABILITY

The data that support the findings of this study are available from the corresponding author upon reasonable request.

REFERENCES

[1] M. Johnson, J. Phys. Chem. B **109**, 14278 (2005).
[2] M. Tanaka, J. Cryst. Growth **278**, 25 (2005).
[3] M. Weisheit, S. Fähler, A. Marty, Y. Souche, C. Poinsignon, and D. Givord, Science **315**, 349 (2007).
[4] S. J. Glass and M. J. Klein, Physical Review **109**, 288 (1958).
[5] E. Fortin and W. M. Sears, J. Phys. Chem. Solids **43**, 881 (1982).
[6] M. Glazov, T. Amand, X. Marie, D. Lagarde, L. Bouet, and B. Urbaszek, Phys. Rev. B **89**, 201302(R) (2014).
[7] A. K. M. Newaz, D. Prasai, J. I. Ziegler, D. Caudel, S. Robinson, R. F. Haglund, Jr., and K. I. Bolotin, Solid State Comm. **155**, 49 (2013).
[8] A. C. Domask, K. A. Cooley, B. Kabius, M. Abraham, and S. E. Mohney, Cryst. Growth Des. **18**, 3494 (2018).
[9] T. E. Kidd, S. Scott, S. Roberts, R. Carlile, P. V. Lukashev, and A. J. Stollenwerk, J. App. Phys. **129**, 174303 (2021).
[10] T. E. Kidd, E. O'Leary, A. Anderson, S. Scott, and A. J. Stollenwerk, Phys. Rev. B **100**, 235447 (2019).
[11] T. E. Kidd, J. Weber, R. Holzapfel, K. Doore, and A. J. Stollenwerk, App. Phys. Lett. **113**, 191603 (2018).
[12] A. J. Stollenwerk, L. Stuelke, L. Margaryan, T. E. Kidd, and P. V. Lukashev, J. Phys. Cond. Matter **33**, 425001 (2021).
[13] Y. Unutulmazsoy, R. Merkle, D. Fischer, J. Mannhart, and J. Maier, Phys. Chem. Chem. Phys. **19**, 9045 (2017).
[14] P. E. Blöchl, Phys. Rev. B **50**, 17953 (1994).
[15] G. Kresse and D. Joubert, Phys. Rev. B **59**, 1758 (1999).
[16] J. P. Perdew, K. Burke, and M. Ernzerhof, Phys. Rev. Lett. **77**, 3865 (1996).
[17] M. Methfessel and A. T. Paxton, Phys. Rev. B **40**, 3616 (1989).
[18] S. Grimme, J. Antony, S. Ehrlich, and H. Krieg, J. Chem. Phys. **132**, 154104 (2010).
[19] MedeA-2.22, Materials Design, Inc., San Diego, CA, USA, 2017.
[20] J. Towns, T. Cockerill, M. Dahan, I. Foster, K. Gaither, A. Grimshaw, V. Hazlewood, S. Lathrop, D. Lifka, G. Peterson, R. Roskies, J. R. Scott, and N. Wilkins-Diehr, Comput. Sci. Eng. **16**, 62 (2014).
[21] T. T. Chen and V. A. Marsocci, J. App. Phys. **43**, 1554 (1972).
[22] V. A. Isnaini, T. Kolonits, Z. Czigány, J. Gubicza, S. Zsurzsa, L. K. Varga, E. Tóth-Kádár, L. Pogány, L. Péter, and I. Bakonyi, Eur. Phys. J. Plus **135**, 39 (2020).
[23] W. Jie, Z. Yang, F. Zhang, G. Bai, C. W. Leung, and J. Hao, ACS Nano **11**, 6950 (2017).
[24] N. M. Parish and P. B. Littlewood, Nature **426**, 162 (2003).
[25] L. Jamilpanah, M. Hajiali, and S. M. Mohseni, J. Magn. Magn. **514**, 167206 (2020).